ISSN : 0974 - 7478 Volume 9 Issue 3

Macromolecules

An Indian Journal

Full Paper

MMAIJ, 9(3), 2013 [91-101]

Toughening poly (trimethylene terephthalate) by maleinized acrylonitrile-butadiene-styrene

Yingbin Liu, Na Li, Mingtao Run*

College of Chemistry and Environmental Science, Hebei University, Baoding 071002, Hebei, (P.R.CHINA)

E-mail : Lhbx@hbu.edu.cn

ABSTRACT

Poly (trimethylene terephthalate) was melt-blended with Maleinized acrylonitrile-butadiene-styrene to enhance its toughness without sacrificing comprehensive performance. The advantage of using ABS-g-MAH is due to its high toughness, good processing properties and higher molecular polarity. The phase morphology, mechanical properties, crystallization behaviors, dynamic mechanical behaviors, rheology, spherulites morphology, thermal stability and thermal aging properties were investigated by scanning electron microscopy (SEM), universal tester, differential scanning calorimetry (DSC), dynamic mechanical analyzer (DMA), capillary rheometer, polarized optical microscopy (POM), thermogravimetric analyzer and color-difference meter, respectively. The results suggest that the dimension of the dispersed phase is lower than 1 μm and the interface between ABS and PTT is unsharp; therefore, ABS is compatible with PTT. With addition of 5%ABS, the yielding strength, breaking strength and impact strength of the blends increase 41.5%, 167% and 200% than those of pure PTT; therefore, ABS can not only greatly toughen PTT but also reinforce PTT to some extent with proper additions. ABS also serves as a nucleating agent for increasing the crystallization rate. The blends show larger storage modulus and higher glass transition temperatures than those of pure PTT. ABS improves the processing property of PTT by increasing the apparent viscosity of the blends. However, the blends of PTT/ABS show decreased thermal aging resistance of the blends.

© 2013 Trade Science Inc. - INDIA

KEYWORDS

Poly (trimethylene terephthalate);
Mechanical properites;
Compatibility;
Thermal aging property;
Polymer blends and alloys.

INTRODUCTION

Poly (trimethylene terephthalate) (PTT) is a linear aromatic polyester which was first produced by Shell Chemicals under the trade name Corterra®[1]. As an engineering thermoplastic, it combines good mechanical properties like poly (ethylene terephthalate) (PET) and good processing properties like poly (butylene terephthalate) (PBT) into one polymer[2,3]. However, PTT has some shortcomings, such as low heat-distortion temperature, low impact strength at low temperature and low viscosity for processing.

Polymer blending is a straightforward, versatile, and inexpensive method for obtaining new materials with bet-

ter properties[4,5]. The important studies on blends of PTT with other polymer include PTT and PEN[6,7], PTT and PBT[8], PTT and PET[9], PTT and EPDM[10,11], PTT and ABS[12], PTT and PS[13], PTT and metallocene LLDPE[14], PTT and PP[15,16], PTT, PBT and PET[17], PTT, EPDM and metallocene PE[18], etc. These blends have some improved properties, such as crystallization, mechanical and rheological properties. In general, the physical, mechanical and rheological properties of immiscible polymer blends depend not only on the constituent polymers but also on the morphologies of the blends. As is well-known, most of these blends are immiscible and incompatible. Some compatibilizers have been used, these include epoxy[12,19], EMP-MA[11], and styrene–butadiene–maleicanhydride (SBM)[12], etc. Xue et al[12] prepared PTT/ABS blends by melt processing with or without epoxy or styrene–butadiene–maleic anhydride copolymer (SBM) as a reactive compatibilizer. They found that PTT is partially miscible with ABS over the entire composition range and both the compatibilizers have compatibilization effects on the blends. As an extensively commercial polymer, Acrylonitrile-butadiene-styrene (ABS) is associated with good processability, dimensional stability and high impact strength at low temperatures[20-22]. ABS is a feasible choice for blending with PTT. In order to improve the miscibility of the polymer matrix with ABS, some maleinized ABS copolymers are usually used as compatibilizers[23].

In this work, PTT was melt-blended with the maleinized ABS (ABS-g-MAH) for improving its toughness, crystallization and rheological properties. Then the influences of ABS-g-MAH concentrations on the phase morphology, mechanical and thermal properties of the blends were also investigated in detail.

EXPERIMENTAL

Raw materials

PTT homopolymer was supplied in pellet form by Shell Chemicals (USA) with an intrinsic viscosity of 0.90 dL/g measured in a phenol/tetrachloroethane solution (50/50, w/w) at 25 °C. The ABS-g-MAH used in our experiment was supplied by Shenyang Siwei Co. Ltd. (China) in pellet form with a density of 1.03 g/cm^3, *MFR*≥7.0 g/min (2160 g, 190 °C) and a grafting ratio of 7-9%.

Blends preparation

PTT and ABS-g-MAH were dried in a vacuum oven at 80 °C and 60 °C respectively for 24 h before preparing the blends. PTT and ABS-g-MAH were mixed together with different weight ratios of ABS-g-MAH/PTT as follows: B0: 0/100; B1: 1/99; B2: 2/98; B3: 3/97; B4: 4/96; B5: 5/95; B7.5: 7.5/92.5; B10: 10/90; B100: 100/0, and then melt-blended in a SHJ-20 type, self-wiping, co-rotating twin-screw extruder (Nanjing Giant Machinery Co., China) operating at a screw speed of 100 rpm, and with temperatures of 210, 235, 250, 255, 255, 250 °C from the first section to the die. The resultant blend ribbons were cooled in cold water, cut up and re-dried before being used in measurements.

Morphology characterization

The morphology of the fracture surface, coated with a thin layer of gold, was observed by a KYKY-2800B type scanning electron microscopy (KYKY Technology Development Ltd., China) at an acceleration voltage of 25 kV. The fracture surfaces were made by impacting the cold blend ribbons in liquid nitrogen.

The spherulites morphology was performed on the polarized optical microscopy (BX-51, Olympus, Japan) with a digital camera system. Samples were pressed between two glass slides with a separation of about 100 μm after first melting on a hot stage at 240 °C for 10 min; they were then cooled to room temperature at a cooling rate of 1 °C/min, with the photographs taken at room temperature.

Differential scanning calorimetry characterization

The melt-crystallization behaviors measurements of various blends were performed on a Diamond DSC instrument (Perkin-Elmer Co., USA), which was calibrated with indium prior to use; the weights of the samples were approximately 7.0 mg. The as-extruded samples were heated to 260 °C at 80 °C/min under nitrogen atmosphere, held for 5 min, then cooled to 0 °C at a constant cooling rate of 10 °C/min, the cooling process was recorded.

Mechanical properties testing

Pure PTT and the blends were prepared into the sheets with the size of 100×100×3.6 mm by a com-

pression molding method at 250 °C; then the sheets were cut into the special splines used in different measurements by a milling machine. The tensile testing method was done according to the ASTM D638 on a Universal Testing Machine (WSM-20, Changchun Intelligent Instrument & Equipment Co. Ltd, China) at room temperature, using the cross-head speed of 10 mm/min. The unnotched Charpy impact tests were carried out according to the ISO 179-1982 standard using splines with size of 60×6×4 mm and an impact tester (JJ-20, Changchun Intelligent Instrument Co. Ltd., China). All the above data reported were the mean and standard deviation from five determinations.

Fourier transform infrared spectroscopy (FTIR) characterization

FTIR spectra were recorded with a Varian-640 spectrophotometer (KBr pellet technique) in the wavenumber from 4000 to 500 cm^{-1} with a resolution of 1 cm^{-1} and averaged over 40 scans.

Rheological performance characterization

The rheological measurements were performed on a XLY-II type capillary rheometer (Jilin University, China) at the temperature range from 230 to 260 °C. The capillary length and diameter are 40 mm and 1 mm respectively. The sample of about 1.5 g was put into the capillary at fixed temperature, held for 10 min, and then measured at the shear stress range of 12-240 kPa. Melt apparent viscosities are calculated by the Hagen-Poiseuille equation[24].

Thermal stability characterization

The decomposition behaviors of the composites were measured on a Pyris 6 type thermogravimetric analyzer (TGA, Perkin-Elmer Co., USA) in the temperature range of 30–700 °C under nitrogen atmosphere at a heating rate of 20 °C/min.

The thermal aging properties of the blends were tested in an oven at 150 °C for 0-20 h aging times. The yellow index (*Yid*), white index (*Wr*) and color difference ($^{3}\%E$) were measured on an auto color-difference meter (SC-800CÿBeijing Kang-guang Co., China).

Dynamic mechanical characterization

The dynamic mechanical properties of the blends were performed on a dynamic mechanical analyzer (DMA, DMA8000, Perkin-Elmer Co., USA) using a single-cantilever vibration mode in the temperature range of 0-170°C at a constant heating rate of 2 °C/min and a frequency of 2 Hz. The standard splines with the size of 10×5×2 mm were made by compression molding method at 250 °C.

RESULTS AND DISCUSSION

Phase morphology

Figure 1 shows the SEM images of fracture surfaces of different samples. It can be seen in Figure 1(a), the fracture surface is not smooth and many strips were observed on the fracture surface, so we concluded that PTT underwent ductile fracture at low temperatures (<-100°C); however, these strips were parallel to each other (parallel to the impact direction) but not regular in the direction, so PTT has somewhat brittleness at low temperatures (<-100°C). In Figure 1(b), the blend with 2% ABS-g-MAH shows a different morphology, in which the surface becomes much rougher and only a few parallel rucks can be observed, indicating that the blend absorbs more energy in breaking than that occurred in pure PTT. In Figure 1(c), the blend with 5% ABS-g-MAH shows no parallel rucks on the rough surface. As shown in Figures. 1(d) and (e), although the surfaces are rough, they become more and more planar with ABS-g-MAH contents increasing from 7.5% to 10%. As the magnification is 500, no dispersed ABS-g-MAH phase can be observed clearly in the image (b-e); while as the magnification is 6,000, the ABS-g-MAH phases are finely dispersed in the matrix with the size lower than 1 μm in Figure 1(f), and the ABS-g-MAH phases do not form sharp boundaries with the matrices. These results suggest that they have some phase interactions.

As we known, if chemical reactions occurred between two polymers in the melt-blending processing, a copolymer may be formed in situ and acted as a compatibilizer. As shown in Scheme 1, when the PTT and ABS-g-MAH were melt blended at 240-255 °C, the ABS-g-MAH having maleic anhydride group was expected to react with the hydroxyl end group of PTT to form a graft copolymer (PTT-g-ABS) at the blend

interface. As a result, the copolymer PTT-g-ABS can be a compatibilizer for PTT and ABS-g-MAH. Similar reactions of hydroxyl group of polyester with anhydrides have been reported[25,26]. However, this reaction is reversible and its equilibrium is highly shifted to the reactant side with increasing temperature[27]. A temperature as high as 255°C certainly corresponds to an equilibrium which is unfavorable for the formation of the PTT-g-ABS. In order to verify whether the graft copolymer is formed in the blends, the FTIR spectra of the blends were characterized and the spectra of PTT, ABS-g-MAH and PTT/ABS10% blend were shown in Figure 2. As seen in Figure 2, the absorption bands of ABS-g-MAH at 1862~1866 cm^{-1} (asymmetric C=O stretching in MAH) and 1782 cm^{-1} (symmetric C=O stretching in MAH) were also observed in the spectra of PTT/ABS10% blend. From the FTIR spectra, we can not be sure whether or how many grafted polyester had formed in the blend. Therefore, FTIR spectroscopy is not successful in identifying the nature of these interactions due to the complexity of the spectra and the overlapping of most of the characteristic peaks.

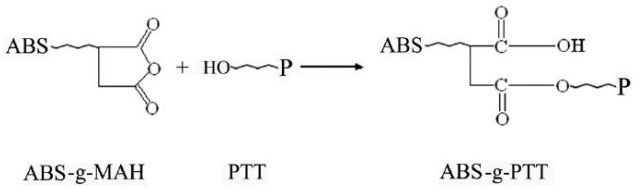

Scheme 1 : Polycondensation reaction between hydroxyl end group of PTT and maleic group of ABS-g-MAH leading to the formation of graft copolymer

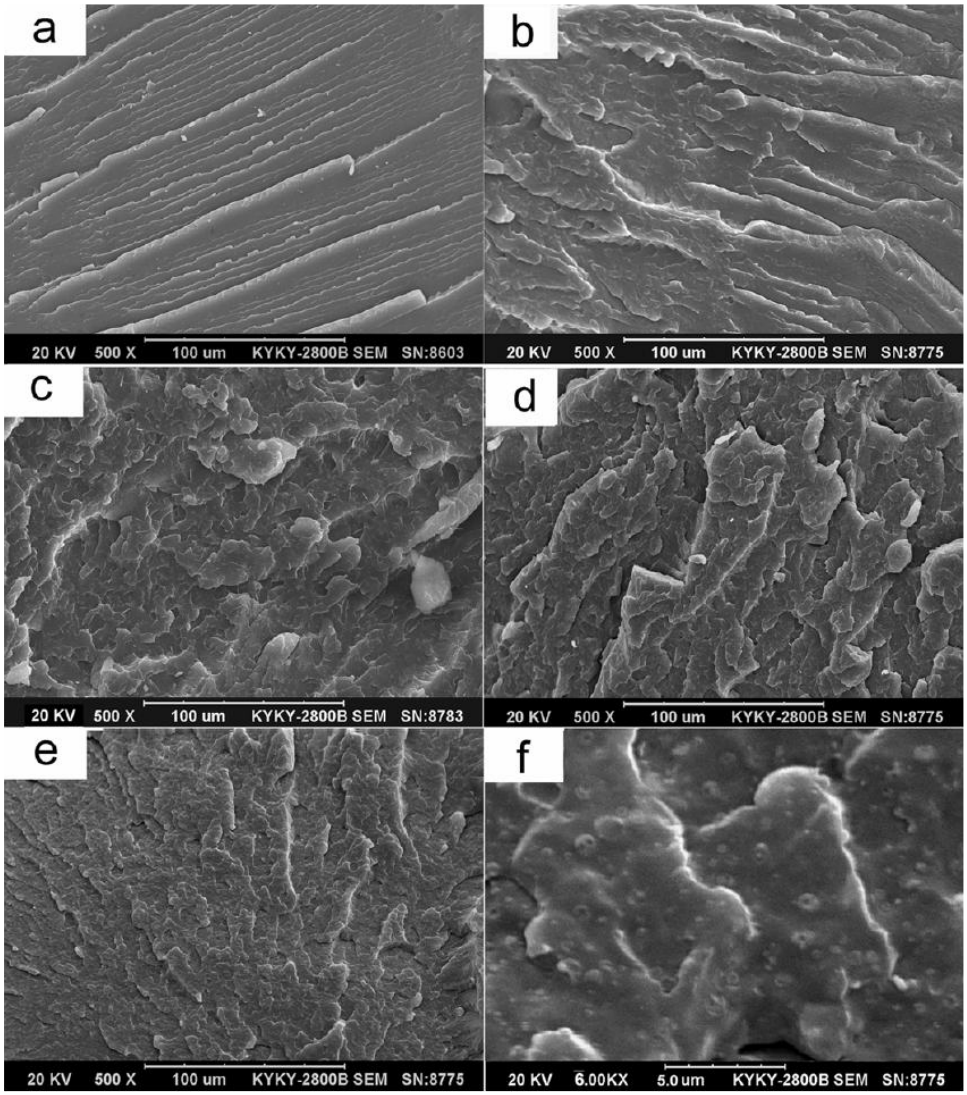

Figure 1 : SEM micrographs of the fracture surface of different PTT/ABS-g-MAH blends. (a)B0, ×500; (b)B2, ×500; (c)B5, ×500; (d)B7.5 ×500; and (e)B10 ×500; (f)B10 ×6000

However, we can also expect intermolecular dipole–dipole interactions and interchange reactions between OH, –COOH and ester groups in the case of maleic anhydride modified polymers and polyesters. If it occurs in the blends, the formed graft copolymer will reduce the interfacial tension and suppress the coalescence behavior; in addition, the presence of the graft copolymer at the blend interface will broaden the interfacial region through the penetration of the copolymer chain segments into the corresponding adjacent phases[28]. On the other hand, the ABS-g-MAH has larger polarities than ungrafted ABS; therefore, the anhydride group in ABS-g-MAH will produce a more polar phase capable of enhanced interactions with the PET phase.

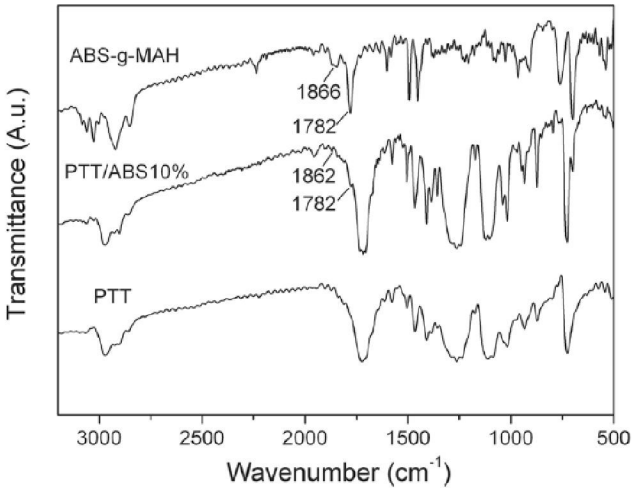

Figure 2 : FTIR spectra of ABS-g-MAH, PTT/ABS10% and PTT

Mechanical properties

As we known, the toughening effect of rubber particles depends on their size, distribution, and particle/matrix interaction[29-30]. These phase-separated particles, especially after the cavitation process, induce large stress concentrations which lead to extensive shear deformation with a high-energy absorbing mechanism[31,32]. Thus, it can be deduced that the mechanical properties of the blends will profit from the small size and uniform distribution of ABS-g-MAH and the strong ABS-g-MAH/PTT interface adhesion.

The mechanical properties were listed in TABLE 1. Pure PTT (B0) has the smallest yield strength, break strength and unnotched impact strength although it has the largest elongation at breaking point among these samples. The blends have larger yielding strength, break strength and unnotched impact strength than those of pure PTT. B4 blend has the largest yielding strength, break strength and tensile modulus; while the B5 blend has the largest unnotched impact strength, which is nearly 3 times than that of neat PTT. The above results suggest that 5% ABS-g-MAH can apparently toughen PTT as well as reinforce PTT. This may be related to three reasons: (1) the hard chain segments in ABS-g-MAH molecules, the acrylonitrile and the styrene chain segments, have larger strength which will reinforce PTT; (2) the soft chain segments in ABS-g-MAH molecules (such as the butadiene chain segments) which has larger impact strength can toughen PTT; (3) the smaller size spherulites in the blends will also be favorable for improving the impact strength of PTT, as shown in the following Figure 3. Of course, we believe that these mechanical results are attributed to the counterbalance of above effects. It can be safely assumed from the above morphological and mechanical properties that PTT will be compatible with ABS-g-MAH.

TABLE 1 : The mechanical properties of different PTT/ABS-g-MAH blends

sample	σ_y [a] (MPa)	σ_b [b] (MPa)	ε [c] (%)	E [d] (MPa)	σ_i [e] (kJ/m^2)
B0	31.3	15.8	289	1462	16.7
B1	37.5	35.9	17.3	1444	25.4
B2	41.3	39.5	14.9	1101	27.7
B3	41.2	39.4	14.7	1186	30.0
B4	44.4	42.9	14.9	990	41.1
B5	44.3	42.2	16.8	1086	50.2
B7.5	41.1	40.3	16.5	1129	40.9
B10	42.2	41.3	12.8	1047	29.5
ABS	44.2	39.4	12.3	1307	73.2

[a] Yielding strength; [b] Break strength; [c] Elongation at breaking point; [d] Tensile modulous; [e] Unnotched impact strength

Spherulites morphology and melt-crystallization behaviors

Figure 3 shows the spherulites morphology of different samples. In Figure 3(a), several large Maltese cross extinctions are observed obviously in pure PTT, and the spherulites are much larger and more perfect than the others shown in the blends of B2, B5 and B10. As shown in Figures. 3(b-d), with increasing ABS-g-MAH content, the spherulites morphology changes sig-

nificantly, i.e., the spherulites dimensions become smaller and smaller, and the perfection becomes worse and worse. For B2, the spherulites dimension is relatively large and the Maltese cross extinction is observed obviously. For B5, the spherulites dimension is significantly reduced, and the Maltese cross extinction becomes weak. For B10, the spherulites dimension is smallest and no clear Maltese cross extinctions can be observed because the spherulites are more disordered and distorted.

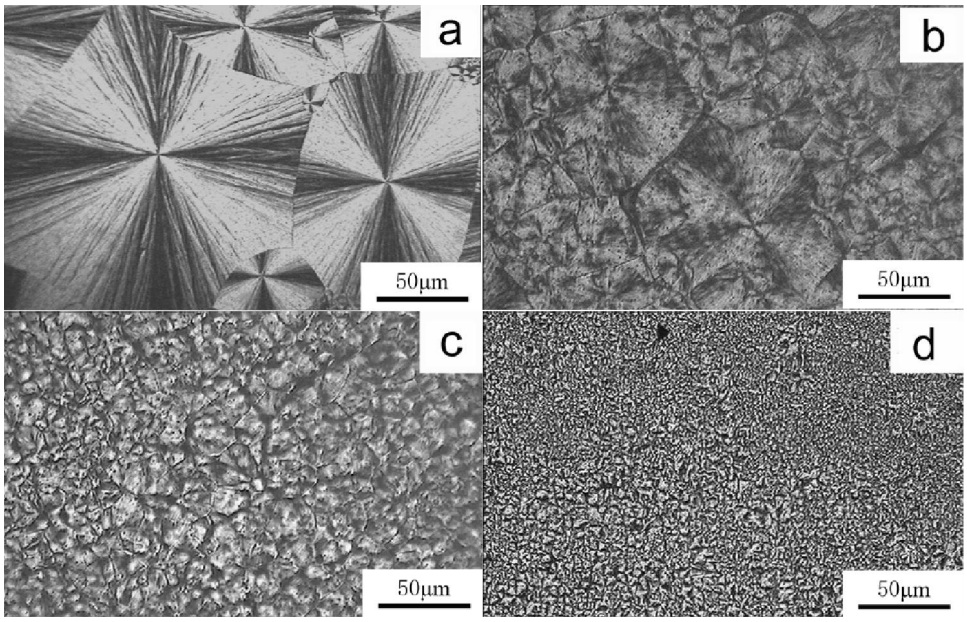

Figure 3 : POM images of different PTT/ABS-g-MAH blends. (a)B0,(b)B2,(c)B5,(d)B10

The melt-crystallization behaviors are usually influenced by the addition of another polymer. Figure 4 shows the DSC cooling curves of eight samples with various ABS-g-MAH contents at the cooling rate of 10 °C/min; the resulting parameters are listed in TABLE 2. According to Figure. 4 and TABLE 2, the crystallization peak temperature (T_{cp}) of neat PTT was the lowest of all samples, and the T_{cp} of the bends shifted to higher temperature with increasing ABS-g-MAH content from 1% to 5%; however, when ABS-g-MAH content increases from 5% to 10%, the T_{cp} values remained unchanged. Moreover, the full width at half-height of the crystallization peak (*FWHP*) decreases as ABS-g-MAH content increased; especially when ABS-g-MAH contents are 7.5% and 10%, the *FWHP* was only 2.8 °C. The crystallization enthalpy ($^3\%H_c$) of neat PTT (B0) was the largest among all the samples. The above phenomena in Figure 3 and Figure 4 suggest two conclusions: (1) ABS-g-MAH served as a nucleating agent for PTT crystallization due to its hard segments in the molecules, such as the acrylonitrile and the styrene segments (SAN); thus it increased both the initial crystallization temperature and the crystallization rate of PTT. The crystallization of different blends (B1-B10) was a nucleation controlled process, and the nuclei in blends may be more active than those in PTT (B0), so the crystal growth process was depressed and the $^3\%H_c$ decreased with increasing ABS-g-MAH content; (2) when ABS-g-MAH content was increased to above 5%, its effect of promoting the crystallization reached saturation.

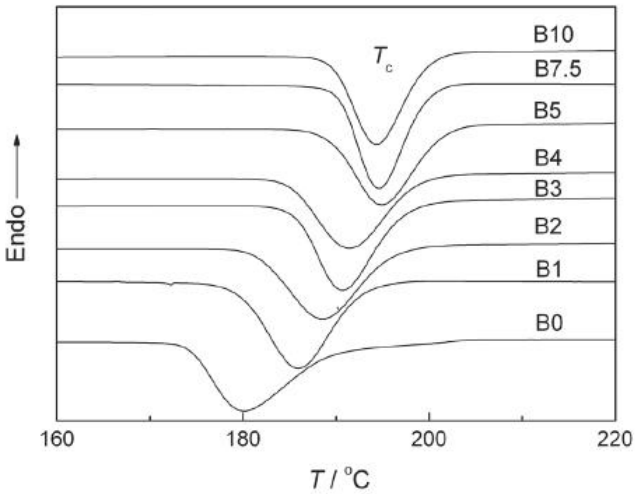

Figure 4 : Crystallization DSC curves of the different blends

TABLE 2 : Crystallization parameters for PTT/ABS-g-MAH blends

Sample	T_{cp} (°C)	ΔH_c [a] (J/g)	*FWHP* (°C)
B0	180.1	-56.8	5.6
B1	185.9	-48.2	4.0
B2	188.6	-46.5	3.8
B3	190.6	-46.6	3.6
B4	191.5	-47.8	4.0
B5	194.9	-45.6	3.8
B7.5	194.6	-48.2	2.8
B10	194.3	-47.8	2.8

[a] the enthalpy has been normalized for PTT contents

Dynamic mechanical properties

The dynamic mechanical behaviors of different blends were investigated from 0°C up to 170 °C and DMA curves are presented in Figure 5 and Figure 6. Figure 5 shows the relationship between the storage moduli (E') with the temperature. In the temperature range of 0-50 °C, it can be seen that E' is changed with different ABS-g-MAH content, i.e., pure ABS-g-MAH has the lowest modulus among all the samples; PTT has a higher storage modulus than that of pure ABS-g-MAH; the storage modulus of all the blends are higher than those of pure PTT and pure ABS-g-MAH, and the blend with 3% ABS-g-MAH has the highest one. These results suggest that ABS-g-MAH has a reinforcement effect on PTT.

In the temperature range of 50-160 °C, the storage modulus of PTT and ABS-g-MAH decreases sharply at around 50 °C and 125 °C; while the storage modulus of the blends decreases slowly with increasing temperature. The slowly decreased modulus of the blends indicates that the hard chain segments of ABS-g-MAH (SAN) greatly impede the movement of PTT chain segments. It can be found that this impeding effect is apparent with even only 1% ABS-g-MAH in the blend. Thus, it can be concluded that there are strong interface interactions between PTT phase and ABS-g-MAH phase, and the chain segments' motions of PTT are hindered by these interactions. At around 125 °C, a small decrease of the modulus can also be observed, especially for the blends with more ABS-g-MAH content, which corresponds to the glass transition of ABS-g-MAH component. When the temperature rises above 70 °C, the $E2$ increases with increasing temperature due to the cold-crystallization of PTT molecules; however, no cold-crystallization behaviors can be observed in the blends.

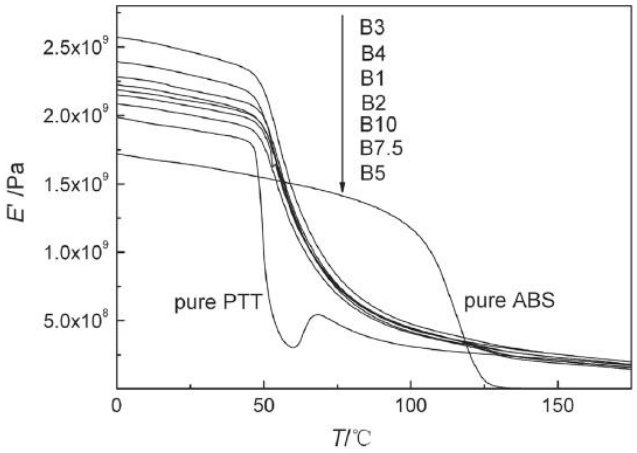

Figure 5 : The curves of storage modulus vs. temperature for different blends

The glass transition of these samples can also be seen in Figure 6, which shows the curves of tanδ vs. temperature. From the results, pure PTT and pure ABS-g-MAH have sharp tanδ peaks at 52.7°C and 129.8 °C respectively. While for different blends, each has two separated weak tanδ peaks at around 69 °C (T_{g1}) and 126 °C (T_{g2}), corresponding to the glass transition of PTT phase and the SAN of ABS-g-MAH phase in the blends respectively. This result indicates that PTT and ABS-g-MAH are compatible in the blend because of their changes on the T_gs values. Even in the blend of B1 that only has 1% ABS-g-MAH, its glass transition

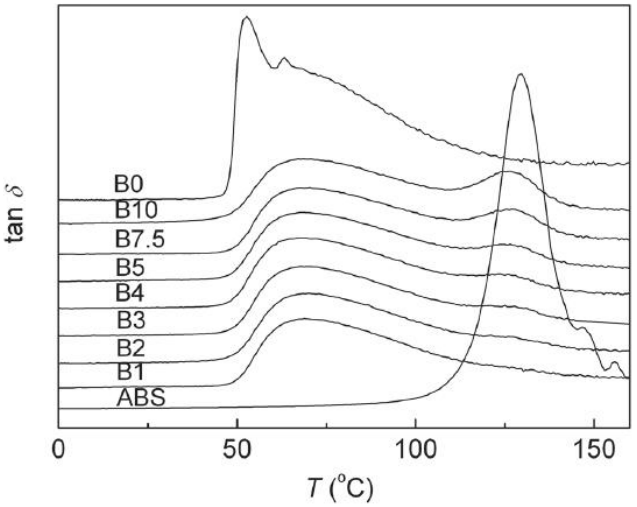

Figure 6 : The curves of tanδ vs. temperature for different blends

peak intensity at about 69 °C decreased greatly; this result clearly show the influence of ABS-g-MAH component on the mobility of the PTT molecular chain segments. It can be seen that the tanδ peaks of ABS-g-MAH phase become larger with increasing ABS-g-MAH content.

Rheological behaviors

Figure 7 shows the rheological curves of different melts at 240°C in the form of the plot of apparent viscosity versus shearing rate. The results show that all the melts are pseudo-plastic fluids for the apparent viscosity decreases greatly with increasing shear rate. The pure ABS-g-MAH has the largest apparent viscosity and the strongest sensitivity to shearing rate among all the samples in low shearing rates, and its apparent viscosity is lower than those of the bends as shearing rate is larger than 450 s^{-1} due to the unentanglement of the molecules. For each blend, their apparent viscosity decreases slowly with increasing shearing rate; while the blends' apparent viscosity increases with increasing ABS-g-MAH contents. Therefore, the increasing viscosity may be favorable for improving the processing property of PTT by adding more than 5% ABS-g-MAH.

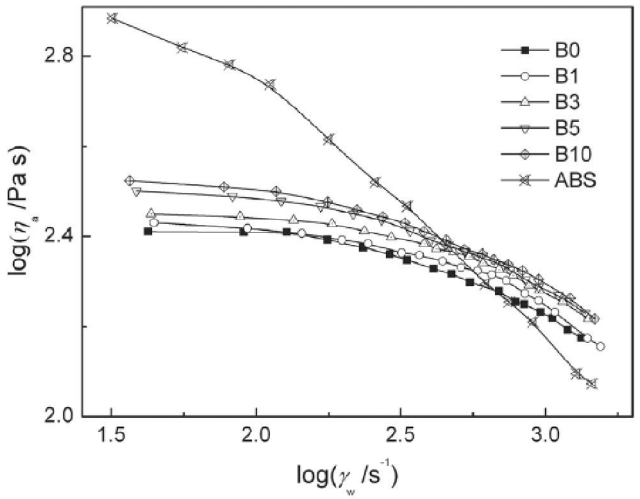

Figure 7 : Plots of logη_a vs. logγ_w

The Non-Newtonian index was calculated and its relationship with ABS-g-MAH content is shown in Figure 8. We can see that *n* is less than 1 for their pseudo-plastic fluid behaviors, and it decreased with increasing ABS-g-MAH content. This result suggests that the pseudoplasticity is increased slightly with increasing ABS-g-MAH content.

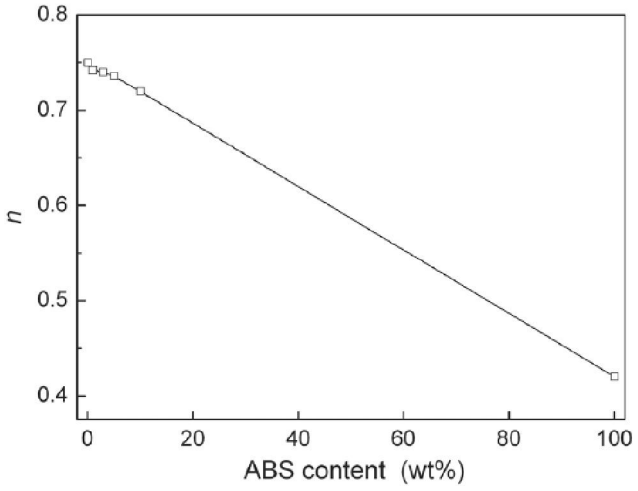

Figure 8 : Relationship between *n* and ABS-g-MAH contents

At different temperatures, the melt apparent viscosity versus ABS-g-MAH content was plotted in Figure 9. It is clear that the melt viscosity increases with increasing ABS-g-MAH content at the same temperature, while it decreases greatly with increasing temperatures from 230 to 260 °C, indicating that the temperature has large influence on the viscosity and it will influence the material processing. The Andrade-Arrhenius equation[33] can be used to illustrate the dependence of the melt apparent viscosity (η_a) on temperatures, and the flow activation energy (ΔE_η) was calculated. ΔE_η values for different blends were 64.4(B0), 63.8(B1), 62.6(B3), 61.9(B5) and 61.3(B10) kJ·mmol^{-1}, respectively. With increasing ABS-g-MAH content, ΔE_η values are slightly decreased, indicating that the blends have smaller dependence of on temperature than that of pure PTT.

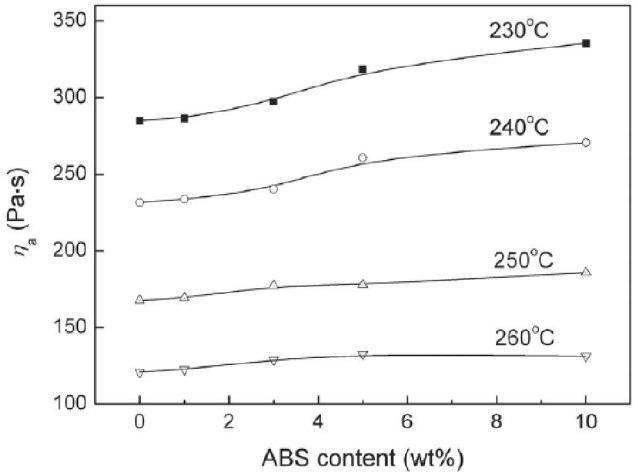

Figure 9 : Relationship between η_a and ABS-g-MAH contents at different temperatures

Thermal stability

Figure 10 shows the TGA results for different blends. A two-stage decomposition of each blend is clearly visible in Figure10. The first stage (50-450°C) is the decomposition of the main chains of PTT and ABS-g-MAH, and the second stage (450-600°C) is the further decomposition of small molecules. With increasing ABS-g-MAH content, the second stage is shifted to higher temperatures because of the polyacrylonitrile in ABS-g-MAH which has higher decomposition temperature. The temperature at weight-loss of 5% ($T_{5\%}$) and the maximum weight-loss rate temperature (T_{max}) are taken as the specific temperature of the degradation process. Apparently, the $T_{5\%}$ and T_{max} of the blends are similar with neat PTT, which are found to around 388±2 °C for $T_{5\%}$, 417±2 °C for T_{max}. These results indicate that the existence of ABS-g-MAH has almost no effect on the thermal stability of the PTT and the blends are surely having similar thermal stability.

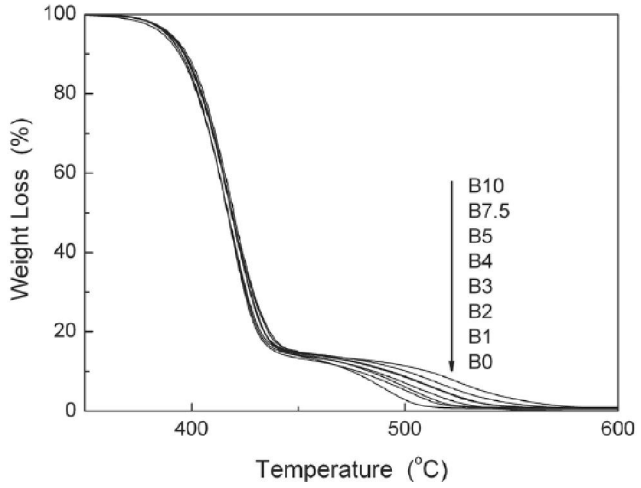

Figure 10 : TGA curves of various PTT/ABS-g-MAH blends

After thermal aging at 150 °C in atmosphere for various hours, the thermal aging properties were tested and the resulting parameters of B0 and B10 were listed in TABLE 3. As shown in TABLE 3, with increasing aging times, the *Yid*, *Wr* and $^{3}\%E$ are gradually increased for B0 sample; however, these parameters are greatly increased for B10 sample. This result suggests that the blend with ABS-g-MAH component has poor thermal aging resistance, which may because of the oxidation behaviors of the double bonds in ABS polymer chain.

TABLE 3 : Thermal aging parameters of B0 and B10

Aging time /h	B0			B10		
	Yid	*Wr*	$\triangle E$	*Yid*	*Wr*	$\triangle E$
0	8.85	56.29	—	23.52	43.73	—
5	9.50	54.76	0.97	47.72	28.82	9.69
10	13.74	50.08	3.63	50.36	27.13	10.84
20	14.88	45.21	7.04	72.7	18.44	17.75

***Yid*: yellow index; *Wr*: white index; $^{3}\%E$: color difference**

CONCLUSION

In this work, ABS-g-MAH was used to toughen PTT by melt-blended with PTT. The results suggest that the blends of PTT and ABS-g-MAH have apparently improved mechanical properties with about 4-5% ABS-g-MAH content. PTT and ABS-g-MAH are compatible. ABS-g-MAH can served as nucleating agent to increase the crystallization of PTT. The addition of ABS-g-MAH has little influence on the rheological behavior of the blends. The thermal aging property of the blends is poor because of the easy oxidation of the double bonds in ABS-g-MAH molecular chains.

ACKNOWLEDGMENTS

The work is supported by the financial support from the Natural Science Foundation of Hebei Province (B2010000219).

REFERENCES

[1] J.R.Whinfield, J.T.Dickson; Improvements relating to the manufacture of highly polymeric substances. 578,079, British **(1941)**.

[2] H.H.Chuah; Orientation and structure development in poly (trimethylene terephthalate) tensile drawing. Macromolecules, **34**, 6985-6993 **(2001)**.

[3] H.A.Khonakdar, S.H.Jafari, A.Asadinezhad; A review on homopolymer, blends, and nanocomposites of poly (trimethylene terephthalate) as a new addition to the aromatic polyesters class. Iran Polym J, **17**, 19-38 **(2008)**.

[4] D.R.Paul, C.B.Bucknall; Polymer Blends. Wiley, New York, **(2000)**.

[5] L.A.Utracki; Polymer Blends Handbook. Kluwer Academic, Dordrecht, **(2003)**.

[6] P.Krutphun, P.Supaphol; Thermal and crystallization characteristics of poly (trimethylene tereph-

thalate)/poly (ethylene naphthalate) blends. Eur.Polym.J, **41**,1561–1568 **(2005)**.

[7] M.T.Run, Y.J.Wang, C.G.Yao, J.G.Gao; Non-isothermal crystallization kinetics of poly (trimethylene terephthalate)/poly (ethylene 2,6-naphthalate) blends. Thermochim Acta, **447**, 13–21 **(2006)**.

[8] P.Supaphol, N.Dangseeyun, P.Srimoaon; Non-isothermal melt crystallization kinetics for poly (trimethylene terephthalate)/poly (butylene terephthalate) blends. Polym Test, **23**,175-185 **(2004)**.

[9] P.Supaphol, N.Dangseeyun, P.Thanomkiat, M.Nithitanakul; Thermal, crystallization, mechanical, and rheological characteristics of poly (trimethylene terephthalate)/poly (ethylene terephthalate) blends. J.Polym.Sci, Part B: Polym Phys, **42**, 676-686 **(2004)**.

[10] H.B.Ravikumara, C.Ranganathaiaha, G.N.Kumaraswamya, S.Thomas; Positron annihilation and differential scanning calorimetric study of poly (trimethylene terephthalate)/EPDM blends. Polymer, **46**, 2372–2380 **(2005)**.

[11] I.Aravinda, P.Alberta, C.Ranganathaiahc, J.V.Kurianb, S.Thomas; Compatibilizing effect of EPM-g-MA in EPDM/poly (trimethylene terephthalate) incompatible blends. Polymer, **45**, 4925-4937 **(2004)**.

[12] M.L.Xue, Y.L.Yu, H.H.Chuah, J.M.Rhee, N.H.Kim, J.H.Lee; Miscibility and compatibilization of poly (trimethylene terephthalate)/acrylonitrile–butadiene–styrene blends. Eur.Polym J, **43**,3826–3837 **(2007)**.

[13] J.M.Huang; Polymer blends of poly (trimethylene terephthalate) and polystyrene compatibilized by styrene–glycidyl methacrylate copolymers. J.Appl.Polym.Sci., **88**, 2247–2252 **(2003)**.

[14] S.H.Jafaria, A.Yavaria, A.Asadinezhada, H.A.Khonakdarb, F.Böáhmec; Correlation of morphology and rheological response of interfacially modified PTT/m-LLDPE blends with varying extent of modification. Polymer, **46**, 5082–5093 **(2005)**.

[15] M.L.Xue, Y.L.Yu, H.H.Chuah, G.X.Qiu; Reactive compatibilization of poly (trimethylene terephthalate)/polypropylene blends by polypropylene–graft–maleic anhydride. Part 1. Rheology, morphology, melting, and mechanical properties. J.Macromol Sci., Part B: Phys., **46**, 387–401 **(2007)**.

[16] S.H.Jafari, A.Kalati-vahid, H.A.Khonakdar, A.Asadinezhad, U.Wagenknecht, D.Jehnichen; Crystallization and melting behavior of nanoclay-containing polypropylene/poly (trimethylene terephthalate) blends. Express Polym lett, **6**,148–158 **(2012)**.

[17] M.T.Run, A.J.Song, Y.J.Wang, C.G.Yao; Melting, crystallization behaviors, and non-isothermal crystallization kinetics of PET/PTT/PBT ternary blends. J.Appl.Polym.Sci, **104**, 3459–3468 **(2007)**.

[18] M.T.Run, H.Z.Song, Y.J.Wang, C.G.Yao, J.G.Gao; Studies on the rheological, phase morphologic, thermal and mechanical properties of poly (trimethylene terephthalate)/ethylene propylene diene monomer copolymer grafted with maleic anhydride/metallocene polyethylene blends. Frontiers of Chem Eng in China, **1**, 238–235 **(2007)**.

[19] M.L.Xue, J.Sheng, H.H.Chuah, X.Y.Zhang; Compatibilization of poly (trimethylene terephthalate)/polycarbonate blends by epoxy. Part 1. Miscibility and morphology. J.Macromol Sci., Part B: Phys., **44**, 317-329 **(2005)**.

[20] S.Hashemi; Effect of temperature on tensile properties of injection moulded short glass fibre and glass bead filled ABS hybrids. Express Polym lett, **2**, 474-484 **(2008)**.

[21] E.M.Araújo, E.Hage Jr, A.J.F.Carvalho; Acrylonitrile-butadiene-styrene toughened nylon 6: the influences of compatibilizer on morphology and impact properties. J.Appl.Polym.Sci., **87**, 842–847 **(2002)**.

[22] M.L.Xue, Y.L.Yu, H.H.Chuah, J.M.Rhee, J.H.Lee; Melting and crystallization behaviors of compatibilized poly (trimethylene terephthalate)/acrylonitrile- butadiene-styrene blends. J.Appl.Polym.Sci, **108**, 3334-3345 **(2008)**.

[23] Jazani O.M., Arefazar A., Jafari S.H., Beheshty M.H., Ghaemi A.: A study on the effects of SEBS-*g*-MAH on the phase morphology and mechanical properties of polypropylene/polycarbonate/SEBS ternary polymer blends. J.Appl.Polym.Sci., **121**, 2680-2687 **(2011)**.

[24] E.Tamaki, A.Hibara, H.B.Kim, M.Tokeshi, T.Kitamori; Pressure-driven flow control system for nanofluidic chemical process. J.Chromatography A, **1137**, 256-262 **(2006)**.

[25] J.Sun, G.H.Hu, M.Lambla, H.K.Kotlar; In situ compatibilization of polypropylene and poly (butylene terephthalate) polymer blends by one-step reactive extrusion. Polymer, **37**, 4119-4127 **(1996)**.

[26] G.H.Hu, T.Lindt; Monoesterification of styrene–maleic anhydride copolymers with alcohols in ethyl benzene: Catalysis and kinetics. J.Polym.Sci.,

Polym.Chem., **31**, 691-700 **(1993)**.

[27] K.Dedecker, G.Groeninckx; Reactive compatibilisation of A/(B/C) polymer blends. Part 1. Investigation of the phase morphology development and stabilisation. Polymer, **39**, 4985-4992 **(1998)**.

[28] L.Boogh, B.Pettersson, J.A.E.Manson; Dendritic hyperbranched polymers as toughеners for epoxy resins. Polymer, **40**, 2249-2261 **(1999)**.

[29] R.Mezzenga, L.Boogh, J.A.E.Manson; A review of dendritic hyperbranched polymer as modifiers in epoxy composites. Compos.Sci.Technol, **61**, 787-795 **(2001)**.

[30] J.Fröhlich, H.Kautz, R.Thomann, H.Frey, R.Mülhaupt; Reactive core/shell type hyperbranched blockcopolyethers as new liquid rubbers for epoxy toughening. Polymer, **45**, 2155-2164 **(2004)**.

[31] J.S.Wu, A.F.Yee, Y.W.Mai; Fracture toughness and fracture mechanisms of polybutylene-terephthalate/polycarbonate/impact-modifier blends. J.Mater.Sci., **29**, 4510-4522 **(1994)**.

[32] G.M.Kim, G.H.Michler; Micromechanical deformation processes in toughened and particle filled semicrystalline polymers: Part 2. Model representation for micromechanical deformation processes. Polymer, **39**, 5699-5703 **(1998)**.

[33] Z.Burkus, F.Temelli; Rheological properties of barley β-glucan. Carbohydrate Polym, **59**, 459-465 **(2005)**.